Soft Matter



PAPER View Article Online
View Journal | View Issue



Cite this: *Soft Matter*, 2020, **16**, 9121

Received 17th July 2020, Accepted 2nd September 2020

DOI: 10.1039/d0sm01311k

rsc.li/soft-matter-journal

Nematic colloids at liquid crystal—air interfaces *via* photopolymerization†

Xiaoshuang Wei, 📵 Nicholas Sbalbi 📵 and Laura C. Bradley 📵 *

We demonstrate the preparation of colloidal crystals at nematic liquid crystal–air interfaces by simultaneous photopolymerization and assembly. Polymer colloids are produced by polymerization-induced phase separation of 2-hydroxyethyl methacrylate in the non-reactive liquid crystal (LC) 4-cyano-4'-pentylbiphenyl (5CB) using an open-cell setup. Colloids adsorbed to the nematic 5CB–air interface form non-close-packed hexagonal crystals that cover the entire interface area. We examine the mechanism of growth and assembly for the preparation of LC-templated interfacial colloidal superstructures.

Introduction

Research at the intersection of interfacial and colloidal sciences has led to the development of two-dimensional (2D) colloid assemblies relevant for applications across diverse fields, such as chemical and biological sensing, 1-3 photonics, 4,5 colloidal lithography, 6,7 and stabilization of soft materials. 8,9 A variety of techniques have been developed to prepare 2D assemblies on solid supports, including sedimentation, 10,11 vertical deposition, 12,13 and spin coating. 2,5 A limitation of colloid assemblies formed on solid substrates is that they are prone to defects and cracks, 14,15 whereas assemblies at fluid interfaces can exhibit long-range order with minimal defects. 16 For colloids trapped at interfaces between two isotropic fluids (e.g. water-air^{3,17,18} and water-oil¹⁹⁻²¹), the organization is dictated primarily by electrostatic 17,22 and capillary 3,24 interactions. Alternatively, liquid crystalline phases introduce additional elastic interactions that enable the preparation of colloidal superstructures with tunable and responsive microstructures. 25,26 Colloids of a critical size, that are either adsorbed to LC-fluid interfaces or embedded in confined LC films, induce director distortions which govern the ensemble structure and placement through minimization of the global elastic energy.27-34

The assembly of 2D colloidal crystals at nematic LC (NLC)-fluid interfaces (*i.e.* 2D nematic colloids) offers opportunities to manipulate structural organization.^{35–38} Most commonly, colloids trapped at NLC interfaces form non-close-packed hexagonal lattices. For example, Gharbi *et al.* assembled surface-functionalized silica particles at NLC-air interfaces by aerosol

 $\label{lem:polymer} Department of Polymer Science \ and \ Engineering, \ University of Massachusetts \ Amherst, \ Massachusetts \ 01003, \ USA. \ E-mail: \ laurabradley@umass.edu$

deposition where the colloidal structure (hexagonal lattices or linear chains) was controlled by varying the colloid density and NLC thickness.³⁹ Smalyukh et al. demonstrated the assembly of monodisperse glycerol droplets trapped at NLC-air interfaces. 40 In this system, glycerol droplets were formed by heating the NLC layer supported on a glycerol subphase to promote diffusion of glycerol into the isotropic LC. Upon subsequent cooling, phase separation and the isotropic-to-nematic transition occur simultaneously producing glycerol droplets that either become adsorbed to the NLC-air interface or settle and recombine with the glycerol subphase.41 The interfacial assembly of the glycerol droplets was established to be governed by repulsive elastic dipole and attractive elastic-capillary interactions. Wang et al. explored interfacial assemblies of sulfuric acid droplets at nematic-air interfaces and correlated the tilt of the repulsive elastic dipole on individual colloids to a variety of lattice and chain-like structures. 42 The stability of the interfacial superstructures (maximum area of 0.1 mm²) was correlated to the total number of droplets demonstrating that long-range attraction in the interfacial assembly arises from many-body elastocapillarity. 42-44

Interfacial nematic colloids prepared by simultaneous growth and assembly, to the best of our knowledge, have only been studied in non-reactive systems. While *in situ* polymerization within NLCs is well established for display applications, ^{45,46} few examples exploit NLCs to template the synthesis of microscopic materials such as rings, ⁴⁷ nanofibers, ⁴⁸ and particles. ⁴⁹ Here, we demonstrate LC-templated growth and interfacial assembly of nematic colloids by photopolymerization of 2-hydroxyethyl methacrylate in 5CB using an open-cell setup. Polymer colloids form by polymerization-induced phase separation and assemble into colloidal crystals at the NLC-air interface. Systematic experiments examine colloid growth and assembly for the preparation of large area, LC-templated colloid assemblies.

 $[\]dagger$ Electronic supplementary information (ESI) available. See DOI: 10.1039/d0sm01311k

Soft Matter Paper

Experimental

Coating glass substrates to induce homeotropic anchoring of 5CB

Glass slides were initially cleaned by 15 minute successive sonications at room temperature in soap water, RO water, and acetone. The glass slides were dried at 80 °C for 20 minutes and then further cleaned by oxygen plasma for 20 minutes. Surface coatings of trichloro(1H,1H,2H,2H-perfluorooctyl)silane (fluorinated silane; 97%, Sigma Aldrich) were prepared by chemical vapor deposition in a low-pressure desiccator for 1 hour at room temperature. Alternatively, surface coatings of octyltrichlorosilane (OTS; 97%, Sigma Aldrich) were prepared by immersing glass slides into a 20 mM solution of OTS in heptane (Fisher Chemical) at room temperature for 30 minutes then rinsing with methylene chloride and drying with nitrogen.

Coating glass substrates to induce planar anchoring of 5CB

Glass slides were initially sonicated with soap water at 60 °C for 30 minutes and then rinsed with RO water followed by isopropyl alcohol. The glass slides were dried at 80 °C for 20 minutes. A final cleaning was performed using a 10 minute UV-ozone treatment. A precursor solution (SE610, Nissan) was spin-coated onto the glass slides at 1500 rpm for 30 seconds. The samples were then cured by heating at 80 °C for 1 minute and then at 250 °C for 60 minutes. Lastly, the resulting polyimide coating was rubbed uniaxially 5 times with velvet to induce oriented planar anchoring.

Photopolymerization of 2-hydroxyethyl methacrylate in 5CB

Reaction solutions were prepared by first mixing 2-hydroxyethyl methacrylate (HEMA; 99%, Sigma Aldrich) and photo-initiator 2-hydroxy-2-methylpropiophenone (HMP; 97%, Sigma Aldrich) at a 10:1 v/v ratio. This precursor solution was then mixed with 4-cyano-4'-pentylbiphenyl (5CB; 98%, Sigma Aldrich). All chemicals were used as received. The homogeneous reaction solutions were pinned in copper TEM grids (G50-Cu, Electron Microscope Science) supported on glass slides functionalized to control the 5CB anchoring condition. A small droplet (1 µL) of the reaction solution was added to each TEM grid, with the excess volume being removed by a glass capillary (10 µL, Drummond Scientific Company). The thickness of the liquid layer was $\sim 40 \mu m$, measured by optical profilometry (Zygo, NewView 7300). All samples were annealed at 40 °C for 10 minutes to remove possible defects. This sample setup, in which the 5CBprecursor mixture was in contact with air, is referred to as the "open-cell" system. "Closed-cell" refers to experiments in which the reaction solution was sandwiched between two glass slides using the TEM grid as a spacer. Photopolymerization was carried out at room temperature by exposing samples to ultraviolet (UV) light at either low power (1.2 mW cm⁻² at 254 nm; Analytik Jena US Model UVP UVGL-55; samples positioned 4 cm below the light) or high power (30 mW cm⁻² at 254 nm; Oriel Instruments Model 97434; samples positioned 1 cm below the light). Substrate temperature variations were less than 3 and 6 °C for the low and high power UV systems, respectively.

Sample characterization

Samples were imaged immediately after photopolymerization using optical microscopy (Zeiss Axioimager M2m). Solution compositions as a function of experiment time (evaporation only or UV exposure) were measured by ¹H NMR spectroscopy (Bruker Avance 500) using acetone-d₆ (99.8%, Acros Organics) as the solvent. For structural analyses of the interfacial colloid assemblies, optical microscopy images were first converted to binary images. Colloid positional and orientational order was analyzed using MATLAB (additional details provided in the ESI†). Optical profilometry (Zygo NewView 7300) was used to measure the thickness of the liquid pinned in the TEM grids (5× magnification) and image the colloids adsorbed to the 5CB-air interface using a cylindrical fit for the baseline correction ($50 \times$ magnification).

Results and discussion

Prior to studying photopolymerization in open-cell 5CB mixtures, we characterized the initial phase (isotropic or nematic)

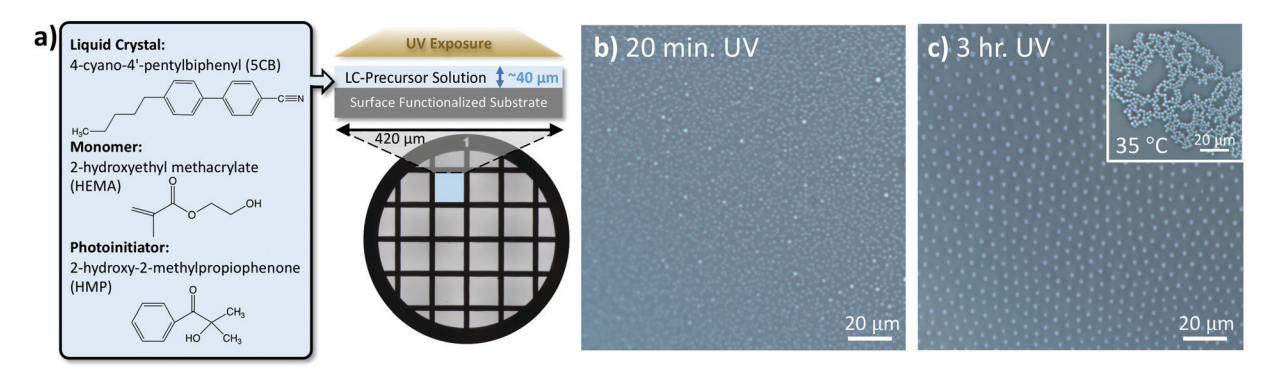


Fig. 1 (a) Schematic of the experimental system in which the reaction solution consisting of 5CB, HEMA (monomer), and HMP (photoinitiator) was pinned in TEM grids supported on glass slides functionalized with fluorinated silane and then exposed to UV light. Photopolymerization at room temperature of reaction solutions with an initial 5CB concentration of 85 vol% produced PHEMA colloids at the air interface. OM images show interfacial colloid assemblies formed by (b) 20 minute and (c) 3 hour UV exposures (1.2 mW cm⁻²). Samples in parts b and c are isotropic and nematic, respectively. The inset in part c shows colloid aggregation after the system was heated above the nematic-to-isotropic transition to 35 °C.

Soft Matter

of the reaction solutions at room temperature (Fig. S1, ESI†). the entire thickness of the solution.

of the reaction solutions at room temperature (Fig. S1, ESI†). Reaction solutions comprising of 5CB, HEMA monomer, and HMP photo-initiator were pinned in TEM grids supported on glass slides functionalized with a fluorinated silane to induce homeotropic anchoring (Fig. 1a). Nematic 5CB has homeotropic anchoring at both the air interface and the substrate surface producing a homogeneously perpendicular director through the thickness of the thin film. Neat 5CB is a well-known thermotropic LC with a nematic-to-isotropic transition temperature of 33 °C, which decreases with decreasing 5CB concentration in solution. Decreasing the 5CB concentration (increasing the monomer concentration) leads to a nematic-to-isotropic transition between 91–94 vol% 5CB. Reaction solutions with ≤91 vol% 5CB are isotropic due to the nematic-to-isotropic transition occurring below room temperature.

We examined photopolymerization in open-cell systems that were initially either nematic or isotropic. Photopolymerization was performed by exposing samples to low power UV light (1.2 mW cm $^{-2}$) and the resulting polymer morphology was imaged by optical microscopy (OM). Systems with an initial nematic phase ($C_{5{\rm CB}}^{\circ}=95$ vol%) remained nematic throughout the entire 3 hour UV exposure, although no polymer structure was observed by OM due to the low final polymer concentration (Table S1 and Fig. S2, ESI†). Systems initially in the isotropic phase ($C_{5{\rm CB}}^{\circ}=85$ vol%) remained isotropic and produced polydisperse colloids after a 20 minute UV exposure. A large population of colloids were observed at the air interface (Fig. 1b), although colloids were also dispersed throughout

the entire thickness of the solution. PHEMA is insoluble in 5CB, therefore the colloids form by polymerization-induced phase separation.⁵⁰ Increasing the UV exposure time led to an isotropic-to-nematic transition between 20 minutes and 1 hour due to a decrease in the monomer concentration associated with both polymerization and monomer evaporation (Fig. S2, ESI†). After the isotropic-to-nematic transition, a non-close-packed hexagonal assembly of monodisperse colloids (Fig. 1c) was assembled over the entire interface area. Optical profilometry confirmed the polymer colloids are pinned to the 5CB-air interface (Fig. S3, ESI†). After a 3 hour UV exposure, all colloids were either incorporated into the assembly at the air interface or settled randomly onto the bottom substrate due to gravity; there were no colloids suspended in the bulk 5CB. The PHEMA nematic colloids at the air interface did not maintain their organization when the system was heated above the nematicto-isotropic transition temperature to 35 °C (Fig. 1c inset). In the isotropic phase, the colloids aggregated due to capillary attraction;52,53 no change in the aggregated structure was observed when the system was cooled back to the nematic phase. The formation of ordered colloid assemblies at the air interface by polymerization-induced phase separation requires the nematic phase to induce organization.

PHEMA nematic colloids at the 5CB-air interface prepared by *in situ* photopolymerization (Fig. 1c) resemble assemblies of pre-formed colloids deposited at nematic-air interfaces.^{39,54} We characterized the organization of the nematic colloids covering the entire interface area (*i.e.* confined) using metrics

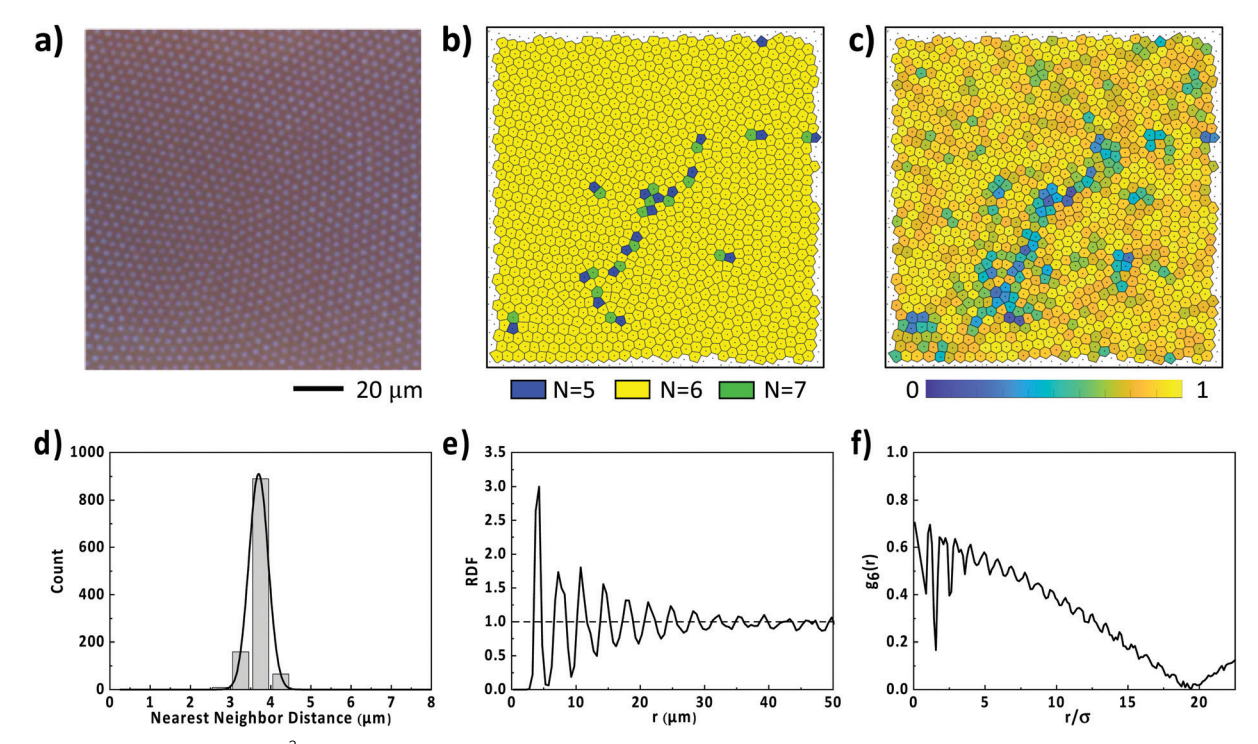


Fig. 2 (a) OM image (135 \times 135 μm^2) of sample D in Table S2 (ESI†) (C_{5CB}° = 85 vol%; 3 hours, low power UV exposure). Colormaps display the (b) number of nearest neighbors and (c) ψ_6 values for all colloids in the analysis area excluding colloids near the image edges; black dots represent the centroids, and the boundary lines represent the Voronoi cells. Plots report the (d) NND distribution with a Gaussian fitting curve, (e) RDF, and (f) ψ_6 orientational correlation function (g_6) in which the x-axis represents the radial distance (r) normalized by the mean NND (σ).

Paper Soft Matter

commonly used throughout the broader scientific community studying colloidal crystals (Fig. 2 and Table S2, ESI†).55 For all samples, the majority of colloids had six nearest neighbors. Lindemann disorder parameters (α), calculated based on the distribution of nearest neighbor distances (NND), are less than the melting criteria of 0.1 for analysis areas of 135 \times 135 μ m² demonstrating local positional order. Additionally, radial distribution functions (RDFs) assessing positional correlations consistently contain multiple peaks reaffirming the assemblies have short-range positional order. Local orientational order was quantified by the local orientational bond order parameter relative to 6-fold symmetry (ψ_6). The average 6-fold bond orientational order parameter, $\langle \psi_6 \rangle$, for all colloids was ≥ 0.69 and the fraction of orientationally ordered colloids (f_6), classified by $\psi_6 > 0.70$, varied between 0.57 to 0.90. The normalized hexatic domain size (Δ_6) , representing the average domain size relative to the average NND, was determined by orientational correlation functions to range from 17 to 45. When the analysis area was increased to $340 \times 340 \ \mu m^2$ (corresponding to 66% of the total interface area), larger variations in colloid spacing result in α values up to 0.13 due to the coexistence of colloidal crystals;³⁵ however, the orientational order is similar to the small area analyses. The compilation of these analyses indicates that the short-range positional and orientational order of the interfacial nematic colloids prepared by photopolymerization is comparable to 2D colloidal crystals produced by alternative fabrication methods.55

Repulsive interactions between the interfacial PHEMA colloids that result in the formation of non-close-packed assemblies with colloid spacings (4-6 µm) several times larger than the colloid diameter (1-2 µm) are due to elastic distortions in the nematic director around each colloid. 32,39,40,42,56 5CB has planar anchoring on PHEMA, and a point defect boojum was observed at the south pole of colloids adsorbed to the air interface (Fig. 3a). Assemblies exhibiting clustering of colloids in certain regions of the interface (i.e. unconfined) were produced when using substrates prepared and stored in ambient conditions for ~ 24 hours before the experiment (Fig. 3b). The long-range attraction between colloids is attributed to a manybody elastic capillary attraction which was originally theoretically described by Pergamenshchik^{43,44} and recently experimentally observed by Wang et al.42 Colloid assemblies filling the entire interface area of the $420 \times 420 \mu m^2$ TEM grid (i.e. confined) were consistently formed using substrates prepared immediately prior to photopolymerization (Fig. 3c). Colloidal crystals were also observed to fill large interface areas of \sim 1.8 mm² (Fig. 3d and Table S3, ESI†).

Prior works established that colloid spacing at nematic-air interfaces increases with increasing colloid size, which is also qualitatively observed in our system (Fig. S4 and Table S4, ESI†). 40,57 Quantifying changes in the colloid size during photopolymerization is below the resolution of OM; therefore, we assessed colloid growth by analyzing the change in NND and colloid count between 2 and 3 hour UV exposures for both confined and unconfined assemblies. For confined assemblies

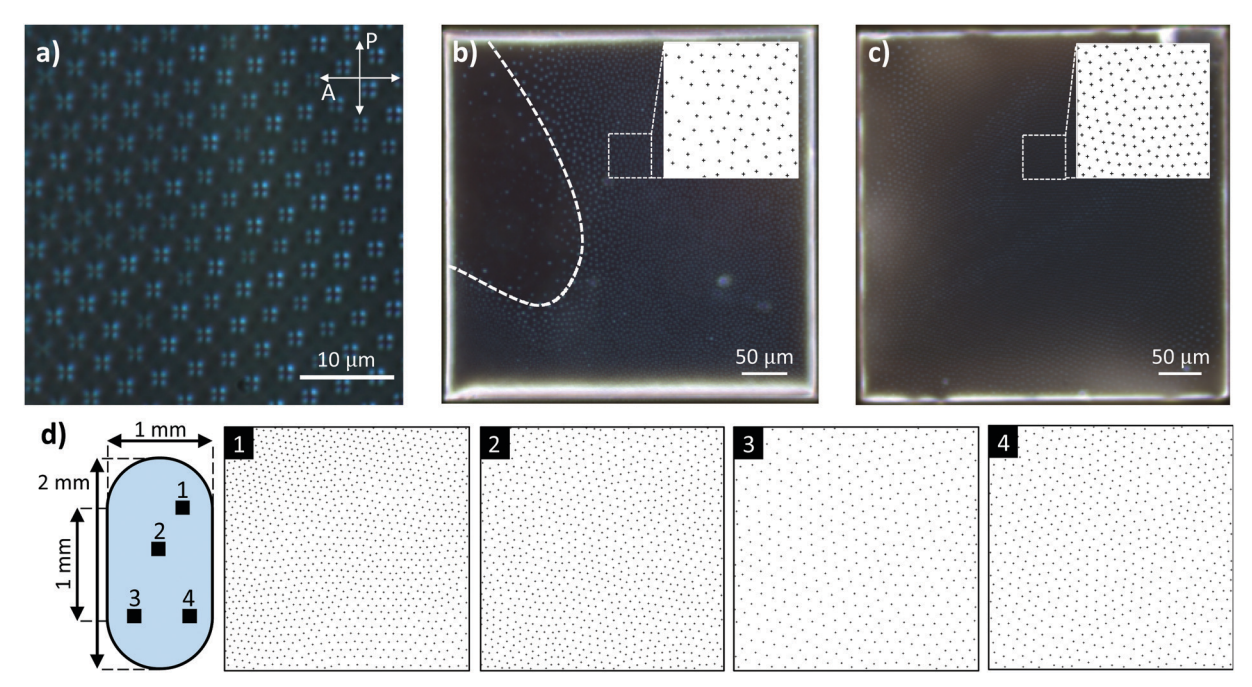


Fig. 3 (a) Polarized optical microscopy image of the point defect boojom at the south pole of PHEMA colloids adsorbed to the nematic 5CB-air interface. OM images of (b) unconfined and (c) confined assemblies in $420 \times 420 \,\mu\text{m}^2$ cells of a TEM grid. Insets in part b and c are both $50 \times 50 \,\mu\text{m}^2$. (d) Confined assemblies are also observed on large area interfaces (\sim 1.8 mm²) using a TEM grid with an oval slot. Four areas (135 \times 135 μ m²) were converted into binary images; the corresponding structural analyses are reported in Table S3 (ESI†). Black crosses in the binary images of parts (b-d) indicate the colloid centroids.

Soft Matter

which fill the entire square-cell of a TEM grid (Fig. 3c), the NND increased by 3 \pm 2% and the colloid count decreased by 6 \pm 3% suggesting no significant change in the number of colloids in the interfacial assembly. We attribute these relatively small changes in NND and colloid count to subtle drift at the nematic-air interface and the confining boundaries of the TEM grid restricting assembly expansion, thus preventing detection of colloid growth. For unconfined assemblies which do not occupy the entire TEM cell (Fig. 3b), the colloid count within the analysis area decreased by 22 \pm 5% corresponding to an increased NND of 12 \pm 3%. Significant expansion of unconfined assemblies between 2 and 3 hour UV exposures suggests continued colloid growth during which there was no significant change in the local positional or orientational order. Alternatively, unconfined colloid assemblies prepared by a 2 hour UV exposure showed no significant change in the assembly structure during a subsequent 1 hour aging without UV light (colloid count decreased by 5 \pm 5% and NND increased by 3 \pm 2%), which confirms colloid growth with continuous UV exposure.

To examine the effect of polymerization kinetics on the preparation of interfacial nematic colloids, photopolymerization in open-cell systems was also carried out using a high power UV exposure (30 mW cm⁻²). For solutions with an initial 85 vol% 5CB, the high power UV exposure resulted in essentially complete monomer conversion within 15 minutes (residual HEMA monomer was less than 0.5 vol%). Immediately after the 15 minute, high power UV exposure, the system was still isotropic and no polymer morphology was observed by OM. After aging the samples 2 hours and 45 minutes to match the 3 hour experiments above, the system had transitioned to the nematic phase and polymer colloids were settled onto the solid support (Fig. S5a, ESI†). Interestingly, there was no colloid assembly at the 5CB-air interface (Fig. S5b, ESI†). The fast polymerization formed an isotropic polymer solution which subsequently phase separated forming colloids in the bulk solution that settled onto the bottom support. Alternatively, in the low power UV experiments (Fig. 1-3), monomer evaporation occurs throughout the photopolymerization and phase separation. We expect that in the low power UV systems, monomer convection due to

evaporation facilitates the adsorption of PHEMA colloids to the air interface where they continue to grow and assemble.

Colloidal crystals produced by photopolymerization in opencell systems were observed only at the air interface. To examine whether the 5CB-air interface is necessary, or whether colloidal crystals can form in the bulk 5CB thin film, 25,27,28 photopolymerization was performed using closed-cell systems in which the reaction solution was sandwiched between two glass slides using a TEM grid as a spacer (Fig. S6, ESI†). Both glass slides were treated with fluorinated silane so that the nematic director was homogenously perpendicular, matching the opencell system. For solutions with an initial 85 vol% 5CB, short 1 minute, low power UV exposures produced a network structure similar to polymer-stabilized LCs. In this closed-cell setup, there was no monomer evaporation which results in a constant 5CB concentration in the system. Increasing the 5CB concentration to 96 vol%, matching the final concentration in the open-cell systems (Fig. 1-3), also resulted in network formation after a 1 minute UV exposure. We hypothesize that the network formation in closed-cell systems, instead of discrete colloids, is associated with confining solid surfaces decreasing mobility in the thin film.⁵⁸ In the open-cell system, we propose the mobility at the fluid 5CB-air interface and slow reaction kinetics facilitate monomer and polymer diffusion promoting the formation of discrete colloids.

Lastly, the effect of substrate surface chemistry on colloid growth and assembly at nematic-air interfaces was examined (Fig. 4). Homogeneously perpendicular directors were established in nematic phases supported on substrates functionalized with either fluorinated silane (as discussed above) or OTS due to a homeotropic anchoring condition; a bent director field was established on rubbed polyimide (PI) due to an oriented planar anchoring condition. All systems produced a population of colloids adsorbed to the air interface. Interestingly, only systems supported on freshly prepared substrates coated with the fluorinated silane produced colloid assemblies that were ordered and covered the entire interface area. We attribute the observed effect of substrate surface chemistry to differences in the 5CB anchoring condition and surface ordering, which is

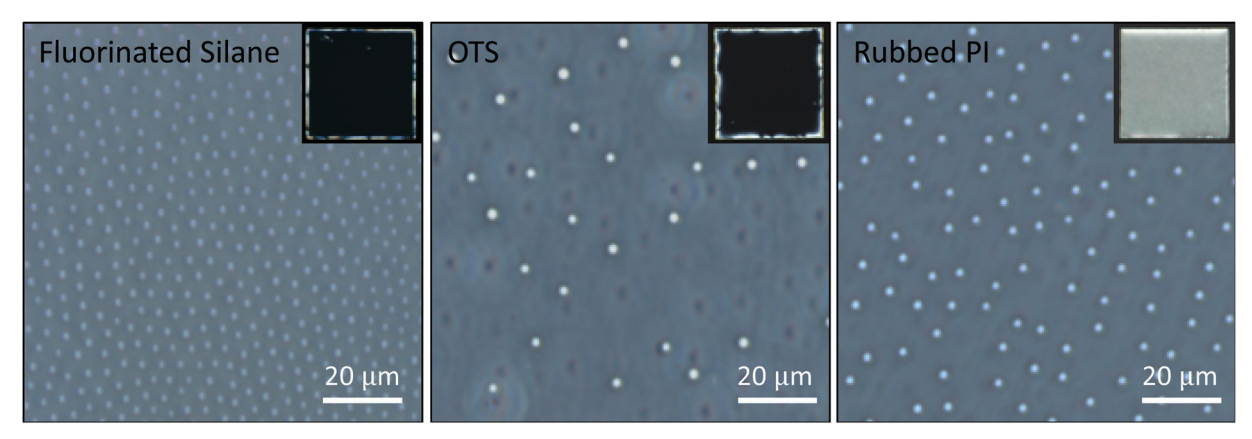


Fig. 4 OM images comparing the effect of substrate surface chemistry on PHEMA colloid assemblies at nematic 5CB-air interfaces prepared by photopolymerization. Insets show the corresponding polarized optical microscopy images of the entire $420 \times 420 \ \mu\text{m}^2$ cell in a TEM grid.

Paper Soft Matter

known to be sensitive to the composition and density of selfassembled monolayers. 59-61 In agreement with prior reports, 40,42 the effect of substrate surface chemistry on colloid assemblies at the air interface indicates elastic distortions throughout the entire nematic thin film contribute to the colloid organization.

Conclusion

In conclusion, we demonstrate the preparation of interfacial nematic colloids by coupling polymerization-induced phase separation with nematic-mediated interfacial assembly in open-cell systems. Photopolymerization of monofunctional (non-crosslinking) 2-hydroxyethyl methacrylate in 5CB formed non-close-packed hexagonal colloidal crystals at the air interface. Organized interfacial assemblies on areas up to $\sim 1.8 \text{ mm}^2$ were demonstrated after the system transitioned from the isotropic to nematic phase. The local positional and orientational order of the PHEMA nematic colloids mirror properties of colloidal crystals prepared by methods requiring independent synthesis and assembly steps. The preparation of polymer colloids at NLCair interfaces by in situ photopolymerization offers future opportunities to leverage LC-templated growth and assembly to produce diverse and functional superstructures.

Conflicts of interest

There are no conflicts of interest to declare.

Acknowledgements

This work was supported by an NSF CAREER Award (No. 1845631). We thank Paul Y. Kim, David A. Hoagland, and Thomas P. Russell for assistance developing the MATLAB code used for structural analyses of the interfacial assemblies. This work was also supported by core facilities in the UMass Amherst Institute for Applied Life Sciences (NMR) and by shared instrumentation in the Department of Polymer Science and Engineering.

References

- 1 S. M. Yang, S. G. Jang, D. G. Choi, S. Kim and H. K. Yu, Small, 2006, 2, 458.
- 2 G. Lawrence, P. Kalimuthu, M. Benzigar, K. J. Shelat, K. S. Lakhi, D. H. Park, Q. Ji, K. Ariga, P. V. Bernhardt and A. Vinu, Adv. Mater., 2017, 29, 1702295.
- 3 J. T. Zhang, L. Wang, D. N. Lamont, S. S. Velankar and S. A. Asher, Angew. Chem., 2012, 51, 6117.
- 4 B. Griesebock, M. Egen and R. Zentel, Chem. Mater., 2002, 14, 4023.
- 5 P. Jiang and M. J. McFarland, J. Am. Chem. Soc., 2004, **126**, 13778.
- 6 B. Fuhrmann, H. S. Leipner, H. R. Höche, L. Schubert, P. Werner and U. Gösele, Nano Lett., 2005, 5, 2524.
- 7 J. Zhao, B. Frank, S. Burger and H. Giessen, ACS Nano, 2011, 5, 9009.

- 8 S. Jiang and S. Granick, Langmuir, 2008, 24, 2438.
- 9 K. L. Thompson, M. Williams and S. P. Armes, J. Colloid Interface Sci., 2015, 447, 217.
- 10 N. D. Denkov, O. D. Velev, P. A. Kralchevsky, I. B. Ivanov, H. Yoshimura and K. Nagayama, Langmuir, 1992, 8, 3183.
- 11 R. Micheletto, H. Fukuda and M. Ohtsu, Langmuir, 1995, **11**, 3333.
- 12 A. S. Dimitrov and K. Nagayama, Langmuir, 1996, 12, 1303.
- 13 V. Kitaev and G. A. Ozin, Adv. Mater., 2003, 15, 75.
- 14 H. Sabouri, K. Ohno and S. Perrier, Polym. Chem., 2015, 6, 7297.
- 15 T. Xia, W. Luo, F. Hu, W. Qiu, Z. Zhang, Y. Lin and X. Y. Liu, ACS Appl. Mater. Interfaces, 2017, 9, 22037.
- 16 E. Sirotkin, J. D. Apweiler and F. Y. Ogrin, Langmuir, 2010, 26, 10677.
- 17 P. Pieranski, Phys. Rev. Lett., 1980, 45, 569.
- 18 N. Vogel, L. de Viguerie, U. Jonas, C. K. Weiss and K. Landfester, Adv. Funct. Mater., 2011, 21, 3064.
- 19 L. Isa, K. Kumar, M. Müller, J. Grolig, M. Textor and E. Reimhult, ACS Nano, 2010, 4, 5665.
- 20 L. M. Goldenberg, J. Wagner, J. Stumpe, B. R. Paulke and E. Görnitz, Langmuir, 2002, 18, 5627.
- 21 S. Reynaert, P. Moldenaers and J. Vermant, Langmuir, 2006, 22, 4936.
- 22 R. Aveyard, J. H. Clint, D. Nees and V. N. Paunov, Langmuir, 2000, 16, 1969.
- 23 B. J. Park, T. Brugarolas and D. Lee, Soft Matter, 2011, 7, 6413.
- 24 D. Ershov, J. Sprakel, J. Appel, M. A. C. Stuart and J. van der Gucht, Proc. Natl. Acad. Sci. U. S. A., 2013, 110, 9220.
- 25 I. Muševič, M. Škarabot, U. Tkalec, M. Ravnik and S. Žumer, Science, 2006, 313, 954.
- 26 A. Nych, U. Ognysta, M. Škarabot, M. Ravnik, S. Žumer and I. Muševič, Nat. Commun., 2013, 4, 1489.
- 27 M. Škarabot, M. Ravnik, S. Žumer, U. Tkalec, I. Poberaj, D. Babič, N. Osterman and I. Muševič, Phys. Rev. E: Stat., Nonlinear, Soft Matter Phys., 2007, 76, 051406.
- 28 M. Škarabot, M. Ravnik, S. Žumer, U. Tkalec, I. Poberaj, D. Babič, N. Osterman and I. Muševič, Phys. Rev. E: Stat., Nonlinear, Soft Matter Phys., 2008, 77, 031705.
- 29 I. I. Smalyukh, Annu. Rev. Condens. Matter Phys., 2018, 9, 207.
- 30 P. Poulin and D. A. Weitz, Phys. Rev. E: Stat., Nonlinear, Soft Matter Phys., 1998, 57, 626.
- 31 I. Muševič, Materials, 2018, 11, 24.
- 32 J. C. Loudet, P. Barois and P. Poulin, *Nature*, 2000, 407, 611.
- 33 Y. Luo, F. Serra and K. J. Stebe, Soft Matter, 2016, 12, 6027.
- 34 C. Peng, T. Turiv, Y. Guo, S. V. Shiyanovskii, Q. H. Wei and O. D. Lavrentovich, Sci. Adv., 2016, 2, e1600932.
- 35 A. B. Nych, U. M. Ognysta, V. M. Pergamenshchik, B. I. Lev, V. G. Nazarenko, I. Muševič, M. Škarabot and O. D. Lavrentovich, Phys. Rev. Lett., 2007, 98, 057801.
- 36 S. I. Paek, S. J. Kim and J. H. Kim, Phys. Rev. E: Stat., Nonlinear, Soft Matter Phys., 2013, 87, 032502.
- 37 I. H. Lin, G. M. Koenig Jr., J. J. de Pablo and N. L. Abbott, J. Phys. Chem. B, 2008, 112, 16552.

38 G. M. Koenig Jr., I. H. Lin and N. L. Abbott, *Proc. Natl. Acad. Sci. U. S. A.*, 2010, **107**, 3998.

Soft Matter

- 39 M. A. Gharbi, M. Nobili, M. In, G. Prévot, P. Galatola, J. B. Fournier and C. Blanc, *Soft Matter*, 2011, 7, 1467.
- 40 I. I. Smalyukh, S. Chernyshuk, B. I. Lev, A. B. Nych, U. Ognysta, V. G. Nazarenko and O. D. Lavrentovich, *Phys. Rev. Lett.*, 2004, **93**, 117801.
- 41 V. G. Nazarenko, A. B. Nych and B. I. Lev, *Phys. Rev. Lett.*, 2001, **87**, 075504.
- 42 N. Wang, J. S. Evans, C. Li, V. M. Pergamenshchik, I. I. Smalyukh and S. He, *Phys. Rev. Lett.*, 2019, 123, 087801.
- 43 V. M. Pergamenshchik, *Phys. Rev. E: Stat., Nonlinear, Soft Matter Phys.*, 2009, **79**, 011407.
- 44 V. M. Pergamenshchik, *Phys. Rev. E: Stat., Nonlinear, Soft Matter Phys.*, 2012, **85**, 021403.
- 45 S. M. Guo, X. Liang, C. H. Zhang, M. Chen, C. Shen, L. Y. Zhang, X. Yuan, B. F. He and H. Yang, ACS Appl. Mater. Interfaces, 2017, 9, 2942.
- 46 H. Khandelwal, A. P. H. J. Schenning and M. G. Debije, *Adv. Energy Mater.*, 2017, 7, 1602209.
- 47 X. Wang, D. S. Miller, E. Bukusoglu, J. J. de Pablo and N. L. Abbott, *Nat. Mater.*, 2016, **15**, 106.
- 48 K. C. K. Cheng, M. A. Bedolla-Pantoja, Y. K. Kim, J. V. Gregory, F. Xie, A. de France, C. Hussal, K. Sun, N. L. Abbott and J. Lahann, *Science*, 2018, **362**, 804.

- 49 X. Wang, E. Bukusoglu and N. L. Abbott, *Chem. Mater.*, 2017, 29, 53.
- 50 I. Hegoburu and E. R. Soulé, Liq. Cryst., 2017, 44, 1525.
- 51 Y. K. Kim, K. R. Raghupathi, J. S. Pendery, P. Khomein, U. Sridhar, J. J. de Pablo, S. Thayumanavan and N. L. Abbott, *Langmuir*, 2018, 34, 10092.
- 52 M. Oettel and S. Dietrich, Langmuir, 2008, 24, 1425.
- 53 V. Garbin, J. C. Crocker and K. J. Stebe, *J. Colloid Interface Sci.*, 2012, 387, 1.
- 54 W. S. Wei, M. A. Gharbi, M. A. Lohr, T. Still, M. D. Gratale, T. C. Lubensky, K. J. Stebe and A. G. Yodh, *Soft Matter*, 2016, 12, 4715.
- 55 P. Bagheri, A. M. Almudallal, A. Yethiraj and K. M. Poduska, *Langmuir*, 2015, 31, 8251.
- 56 Y. K. Kim, X. Wang, P. Mondkar, E. Bukusoglu and N. L. Abbott, *Nature*, 2018, 557, 539.
- 57 T. Yamamoto and M. Yoshida, Appl. Phys. Express, 2009, 2, 101501.
- 58 D. Wang, R. Hu, J. N. Mabry, B. Miao, D. T. Wu, K. Koynov and D. K. Schwartz, *J. Am. Chem. Soc.*, 2015, **137**, 12312.
- 59 B. H. Clare, K. Efimenko, D. A. Fischer, J. Genzer and N. L. Abbott, *Chem. Mater.*, 2006, 18, 2357.
- 60 O. M. Roscioni, L. Muccioli and C. Zannoni, ACS Appl. Mater. Interfaces, 2017, 9, 11993.
- 61 X. Feng, A. Mourran, M. Möller and C. Bahr, *Soft Matter*, 2012, **8**, 9661.